Electronic Supplementary Material (ESI) for ChemComm.

Anthracene-based azo dyes for photo-induced proton-coupled electron transfer

Contents

NMR spectra

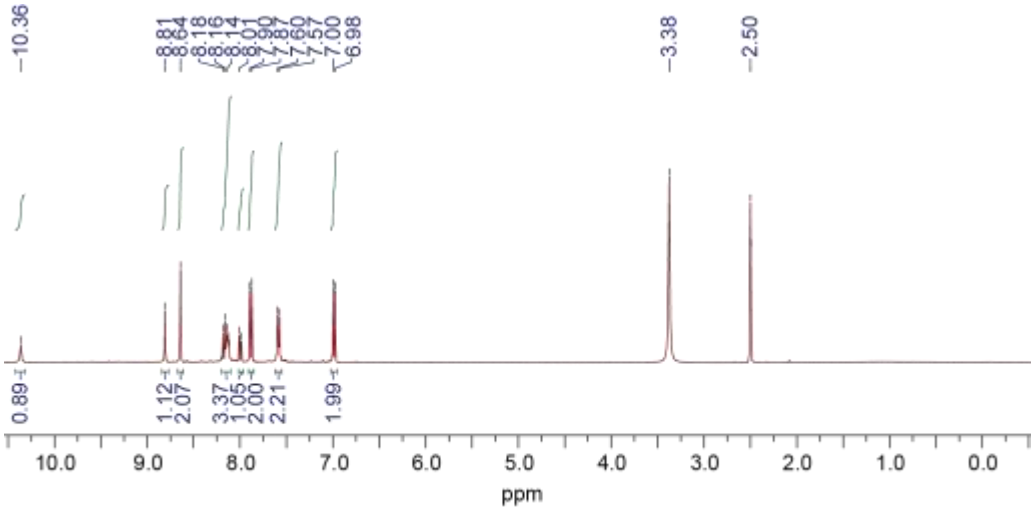

Figure S1. ^{1}H NMR of azo-OH (400 MHz, DMSO) δ 10.36 (s, 1H), 8.81 (s, 1H), 8.64 (s, 2H), 8.25 – 8.05 (m, 3H), 8.00 (d, *J* = 9.1 Hz, 1H), 7.88 (d, *J* = 8.8 Hz, 2H), 7.59 (d, *J* = 9.7 Hz, 2H), 6.99 (d, *J* = 8.8 Hz, 2H).

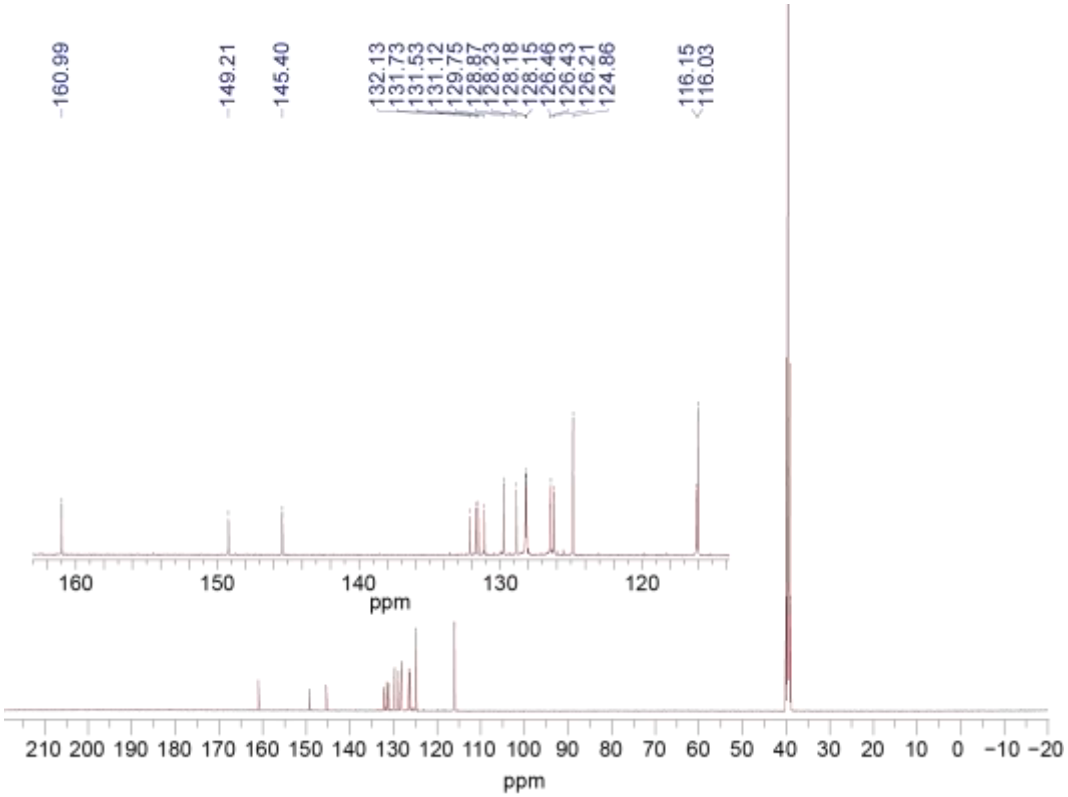

Figure S2. ^{13}C NMR of azo-OH (126 MHz, DMSO) δ 160.99, 149.21, 145.40, 132.13, 131.73, 131.53, 131.12, 129.75, 128.23, 128.18, 128.15, 126.46, 126.43, 126.21, 124.86, 116.15, 116.03

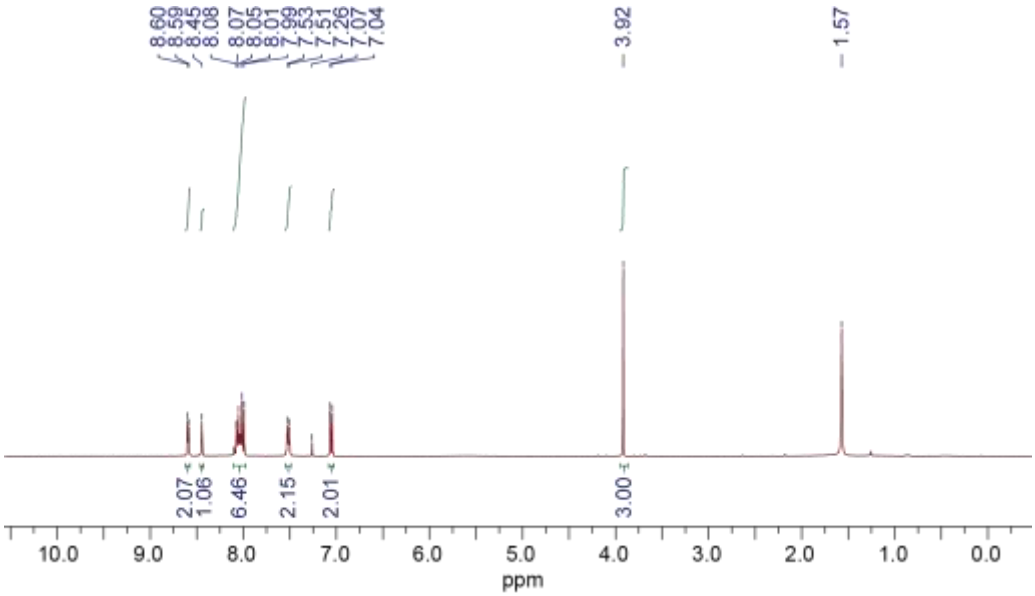

Figure S3. ^{1}H NMR of azo-OMe (400 MHz, $CDCl_3$) δ 8.59 (d, *J* = 4.6 Hz, 2H), 8.45 (s, 1H), 8.12 – 7.96 (m, 6H), 7.52 (d, *J* = 9.7 Hz, 2H), 7.06 (d, *J* = 9.0 Hz, 2H), 3.92 (s, 3H).

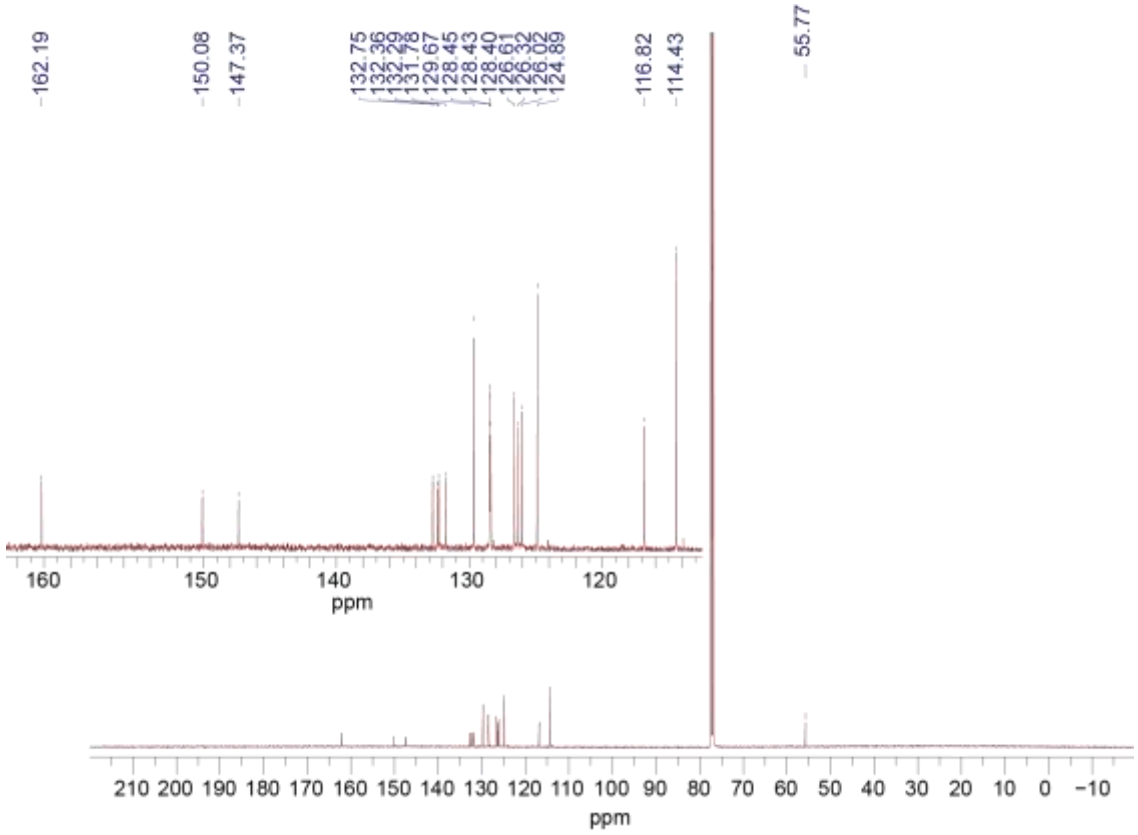

Figure S4. ^{13}C NMR of azo-OH (126 MHz, $CDCl_3$) δ 162.19, 150.08, 147.37, 132.75, 132.36, 132.29, 131.78, 129.67, 128.45, 128.43, 128.40, 126.61, 126.32, 126.02, 124.89, 116.82, 114.43, 55.77

UV-Vis spectra

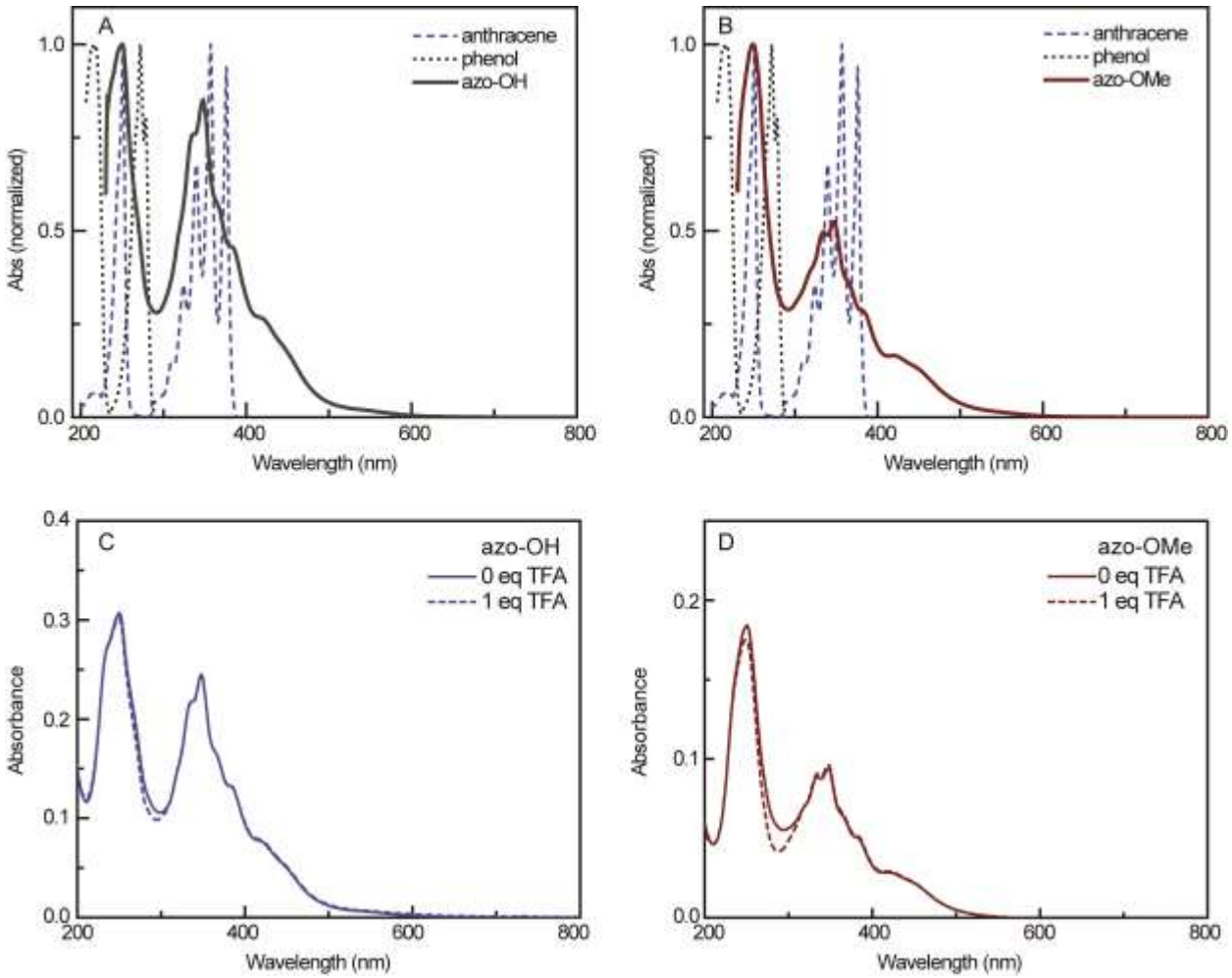

Figure S5. Normalized absorbance spectra of anthracene, phenol, azo-OH (*A*), and azo-OMe (*B*). Absorbance spectra of azo-OH (*C*) and azo-OMe (*D*) in the absence of TFA (*solid*) and presence of 1 eq TFA (*dashed*).

Cyclic Voltammetry and Differential Pulse Voltammetry

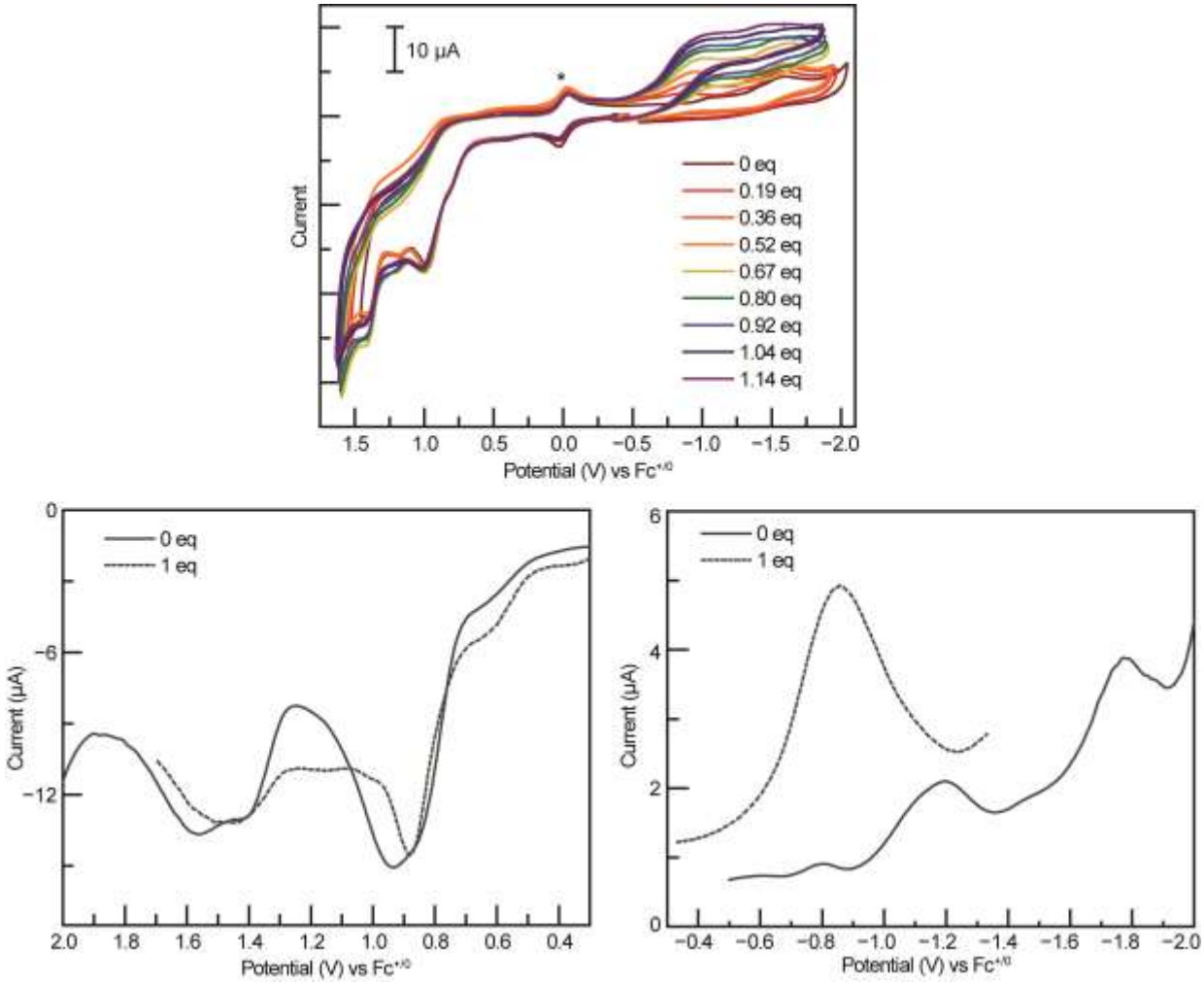

Figure S6. Cyclic voltammograms of 0.5 mM azo-OH (*top*) in 100 mM $TBAPF_6$ in acetonitrile at scan rate = 100 mV/s with additions of TFA. Differential pulse voltammograms of 0.5 mM azo-OH oxidation (*bottom, left*) and reduction (*bottom, right*). The star notes $Fc^{+/0}$ couple.

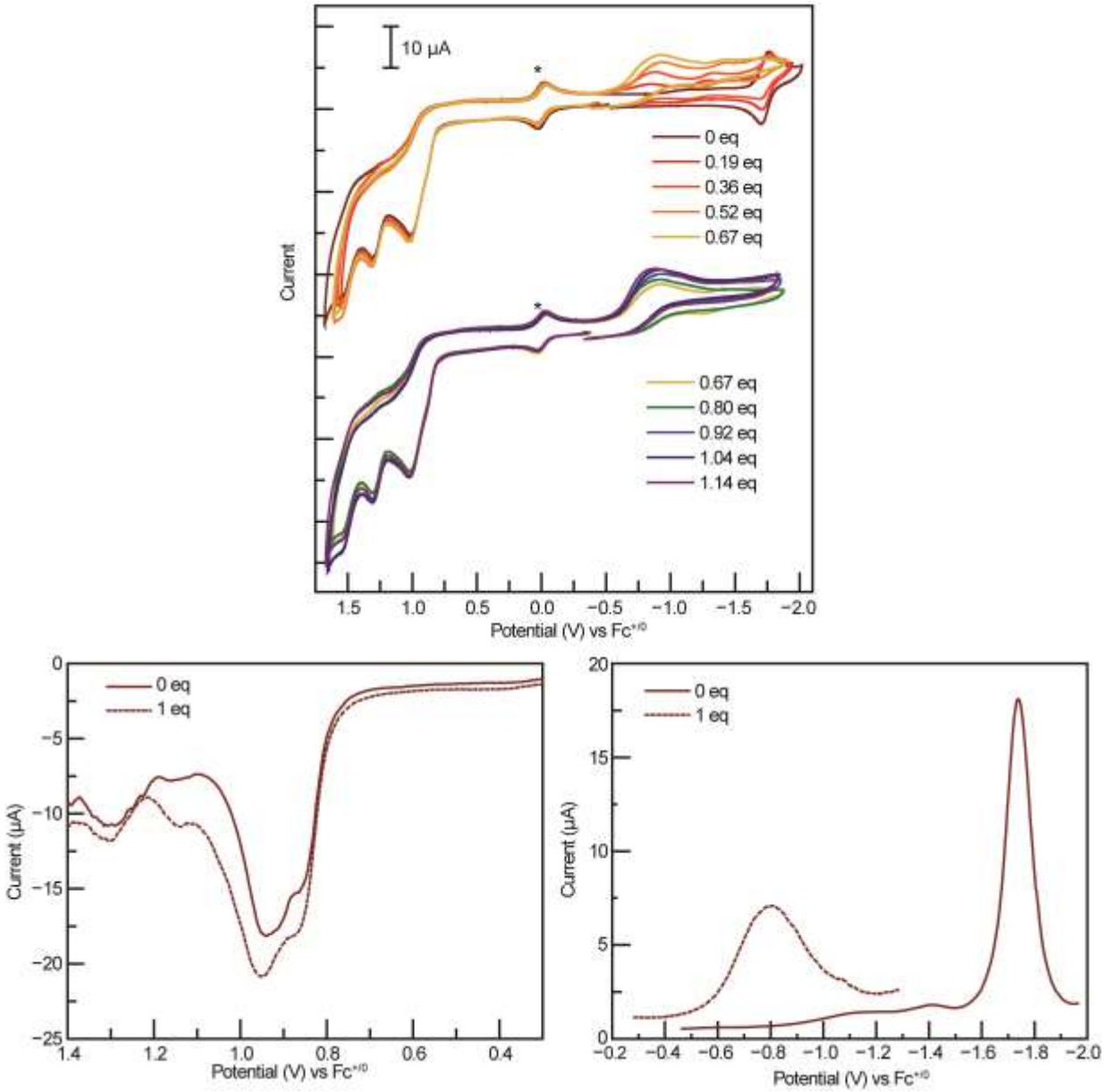

Figure S7. Cyclic voltammograms of 0.5 mM azo-OMe (*top*) in 100 mM $TBAPF_6$ in acetonitrile at scan rate = 100 mV/s with additions of TFA. Differential pulse voltammograms of 0.5 mM azo-OMe oxidation (*bottom, left*) and reduction (*bottom, right*). The star notes $Fc^{+/0}$ couple.

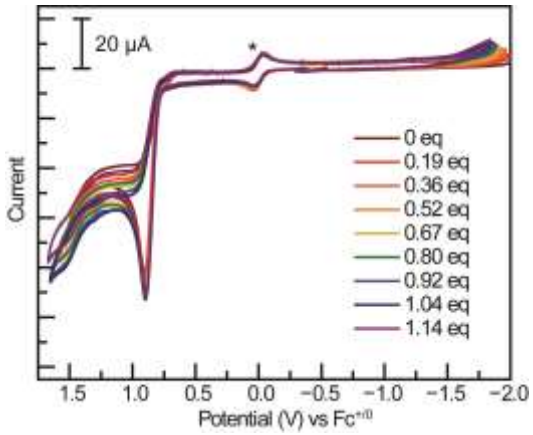

Figure S8. Cyclic voltammograms of 0.5 mM anthracene in 100 mM $TBAPF_6$ in acetonitrile at scan rate = 100 mV/s with additions of TFA. The star notes $Fc^{+/0}$ couple.

Spectroelectrochemistry

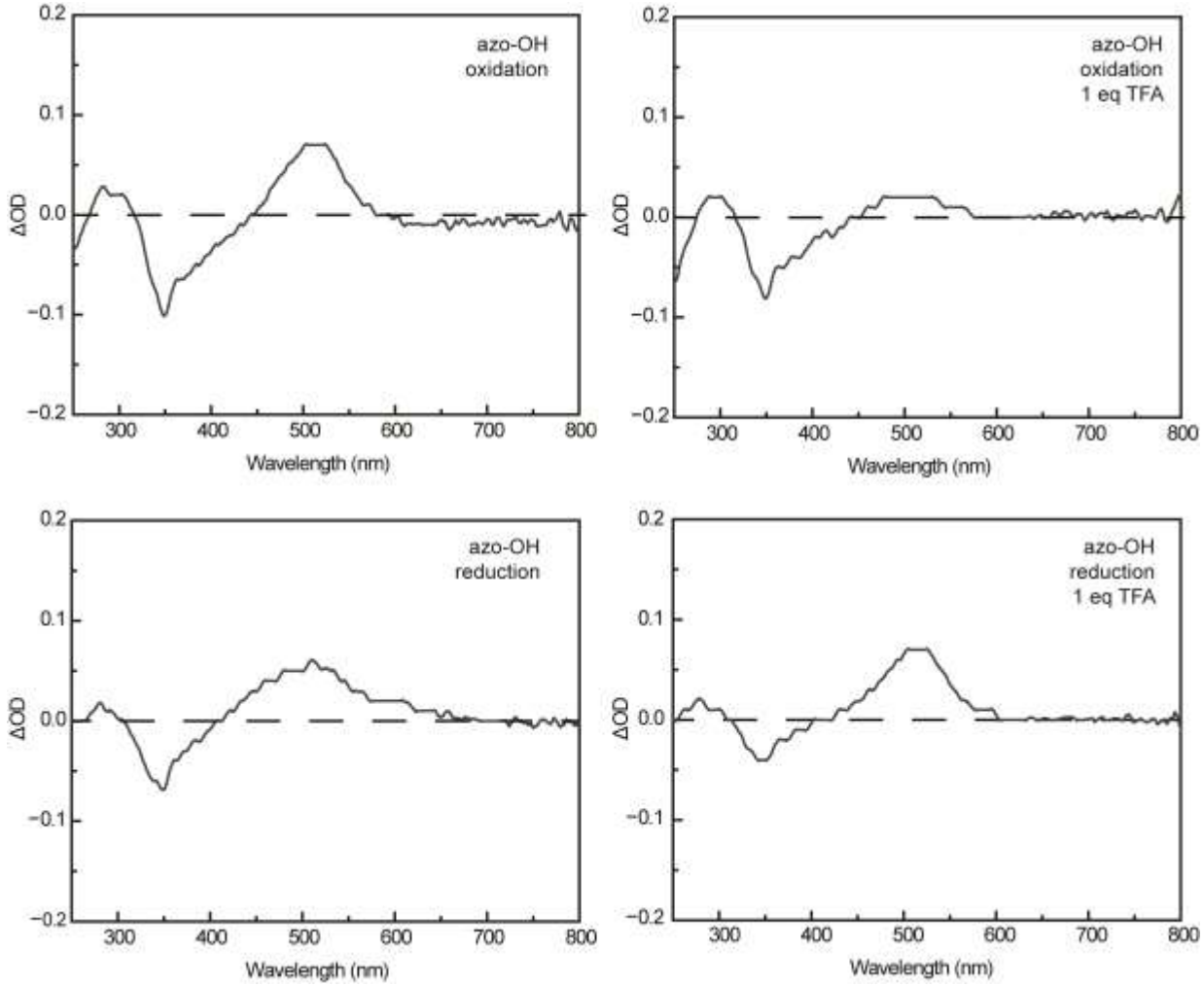

Figure S9. Spectroelectrochemical spectra of 18 µM of azo-OH in 100 mM $TBAPF_6$ in acetonitrile at 1 V vs $Fc^{+/0}$ (*top*) with 0 eq TFA (*left*) and 1 eq TFA (*right*), at −1 V vs $Fc^{+/0}$ with 0 eq TFA (*bottom left*), and at −0.8 V vs $Fc^{+/0}$ with 1 eq TFA (*bottom right*).

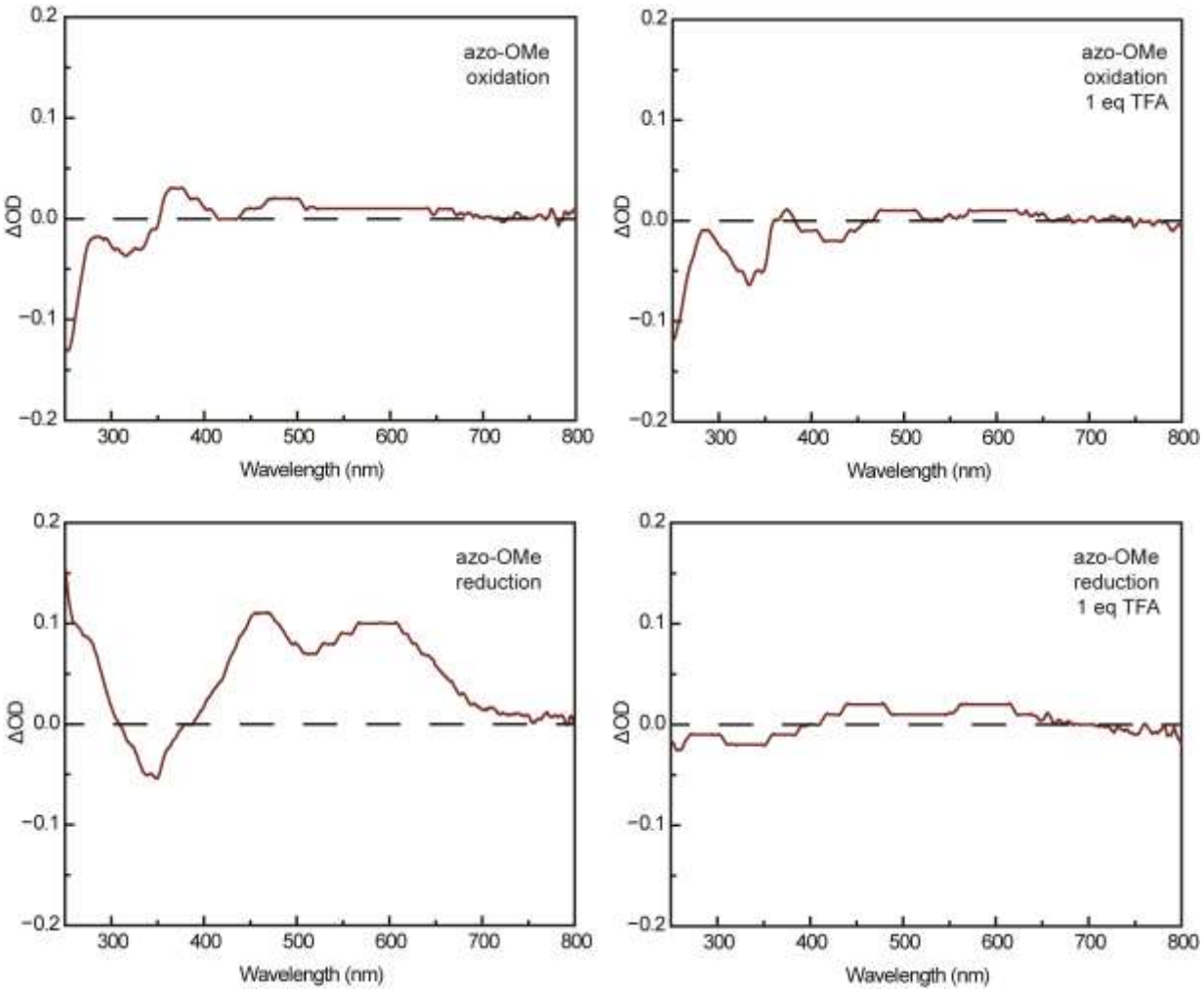

Figure S10. Spectroelectrochemical spectra of 50 µM of azo-OMe in 100 mM $TBAPF_6$ in acetonitrile at 0.9 V vs $Fc^{+/0}$ (*top*) with 0 eq TFA (*left*) and 1 eq TFA (*right*), at −1.7 V vs $Fc^{+/0}$ with 0 eq TFA (*bottom left*), and at −0.8 V vs $Fc^{+/0}$ with 1 eq TFA (*bottom right*).

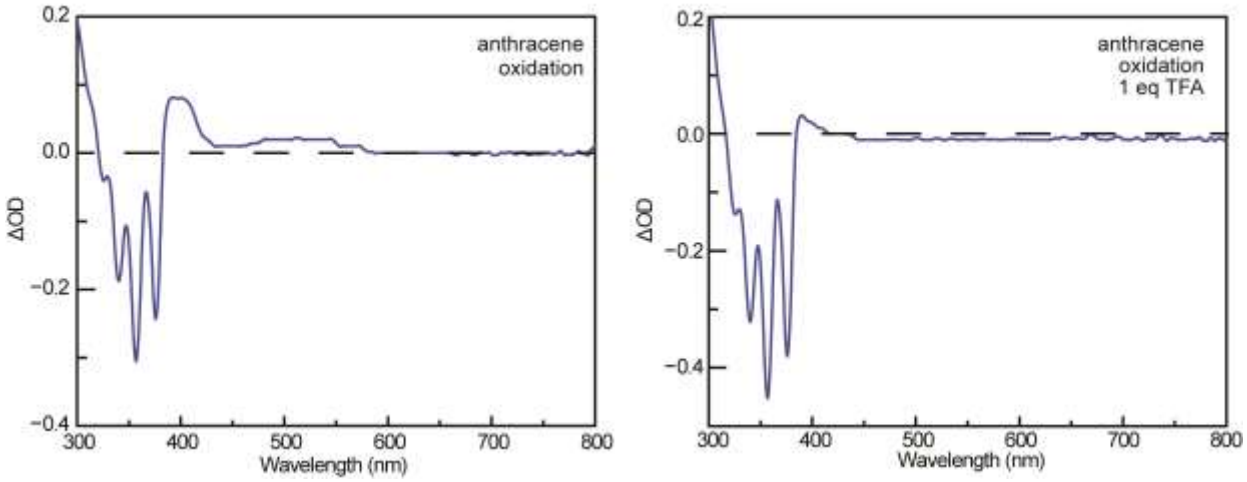

Figure S11. Spectroelectrochemical spectrum of 78 µM of anthracene in 100 mM $TBAPF_6$ in acetonitrile at 0.9 V vs $Fc^{+/0}$ with 0 eq TFA (*right*) and 1 eq TFA (*left*).

Transient Absorption Spectroscopy

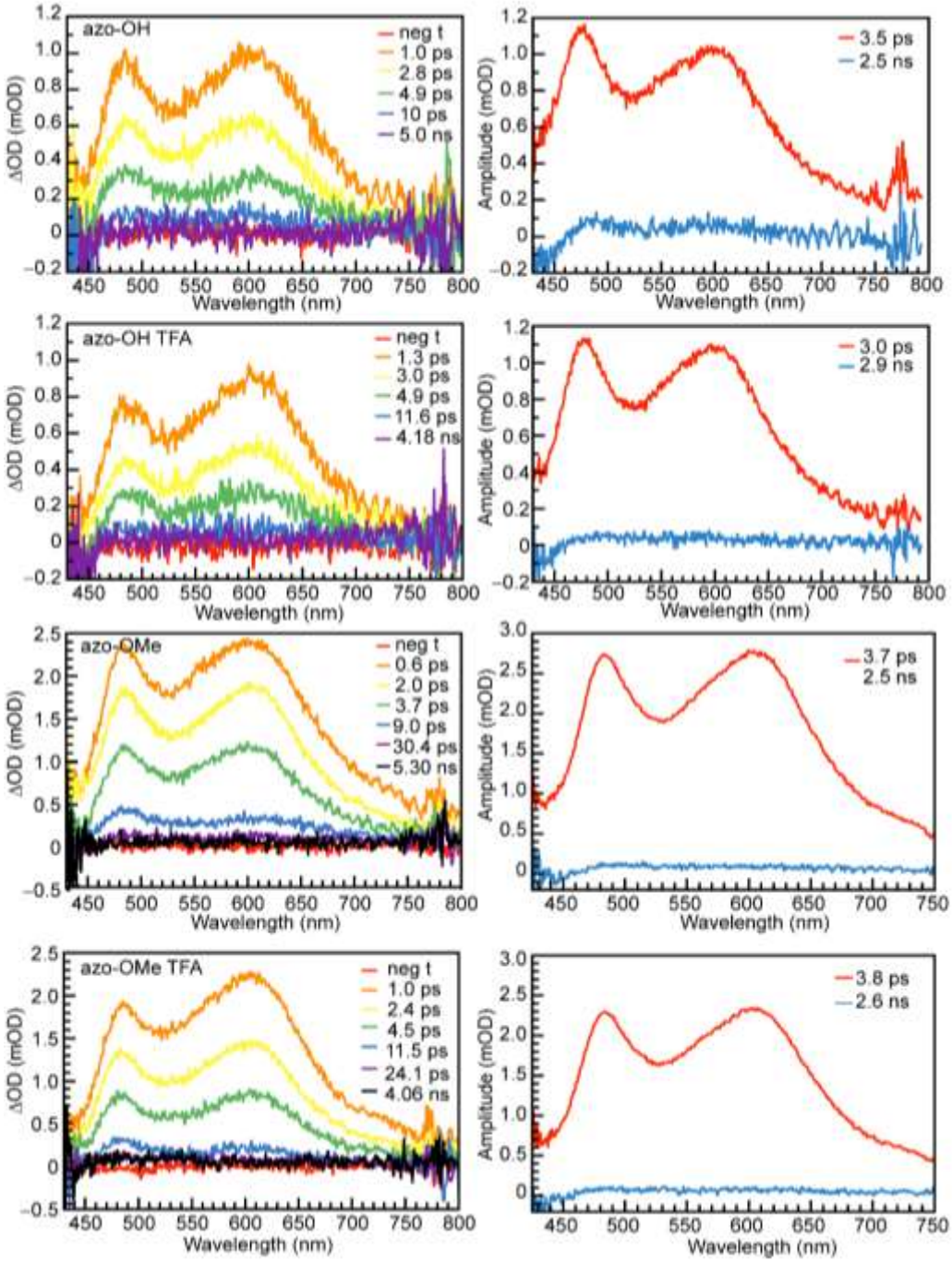

Figure S12. TA Overlay of transient absorption spectra for azo-OMe and azo-OH with 0 or 5 eq TFA. Samples were prepared to 30 μM under an inert nitrogen environment in a 2-mm quartz high-vacuum cuvette. Samples were excited at 370 nm. UV-visible spectra taken before and after TA showed no degradation of the dyads.

DFT & TDDFT Results

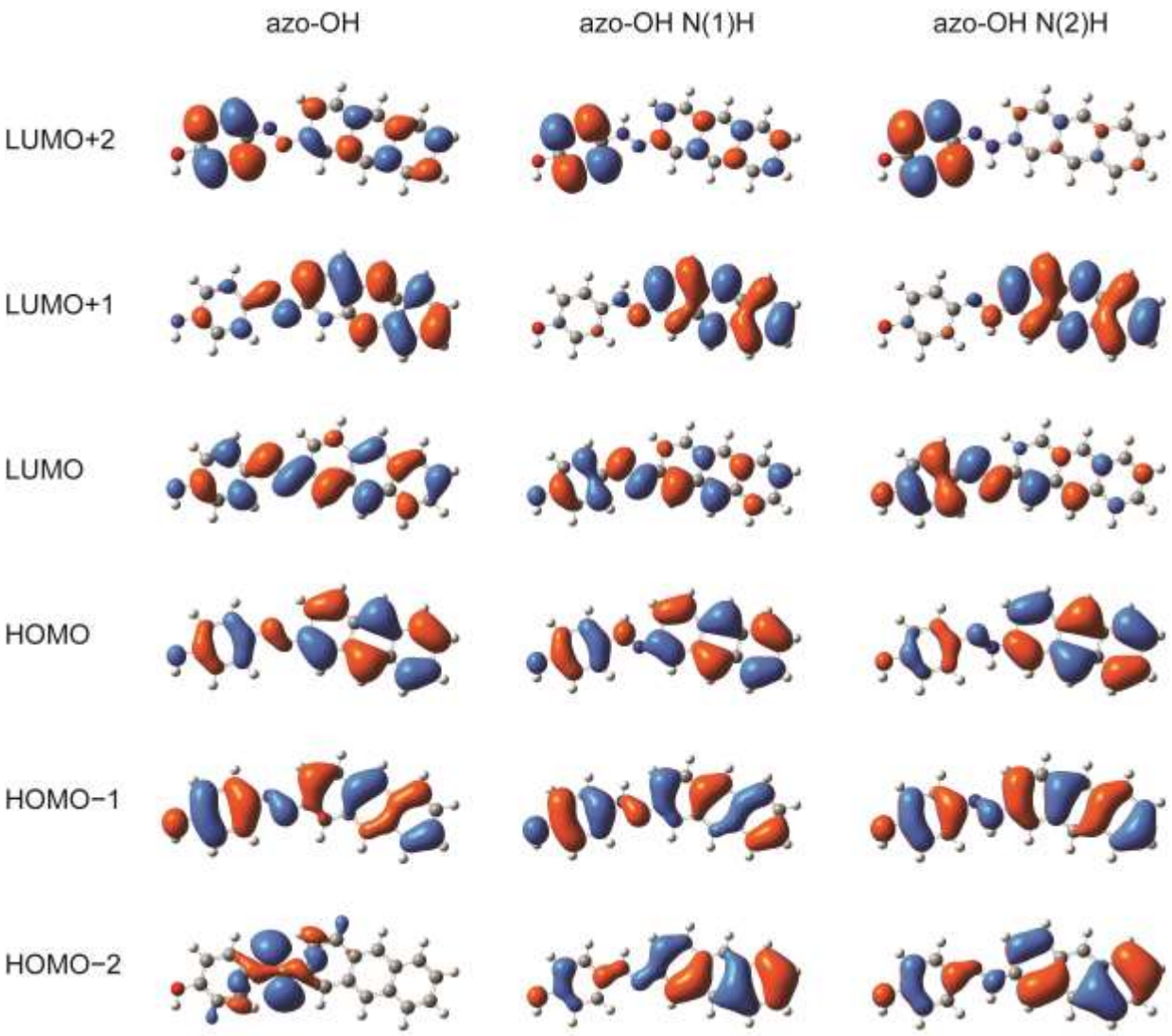

Figure S13. Visualized molecular orbitals of azo-OH protonated at both the phenol-adjacent (N(1)) and anthracene-adjacent (N(2)) azo positions.

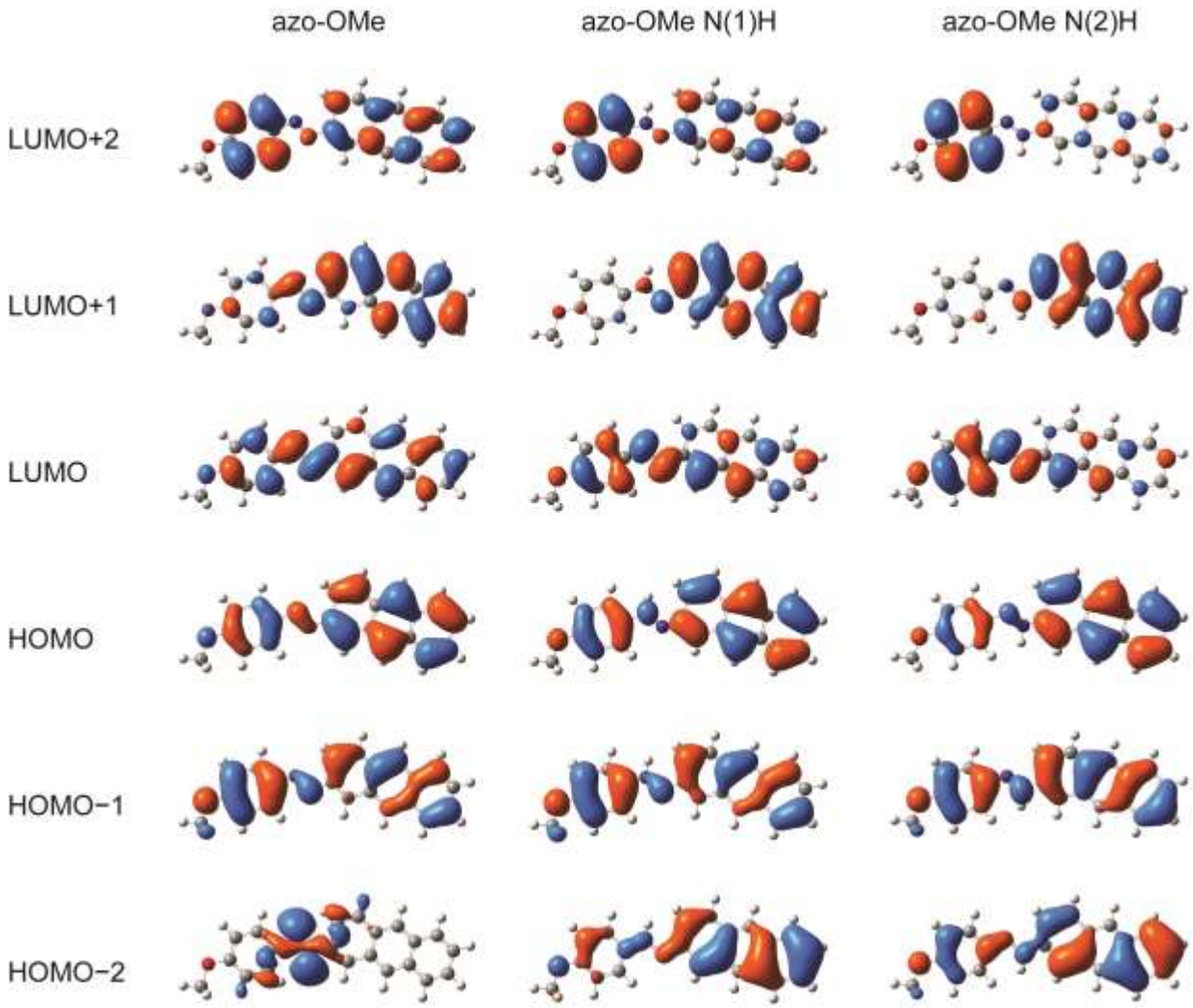

Figure S14. Visualized molecular orbitals of azo-OMe protonated at both the phenol-adjacent (N(1)) and anthracene-adjacent (N(2)) azo positions.

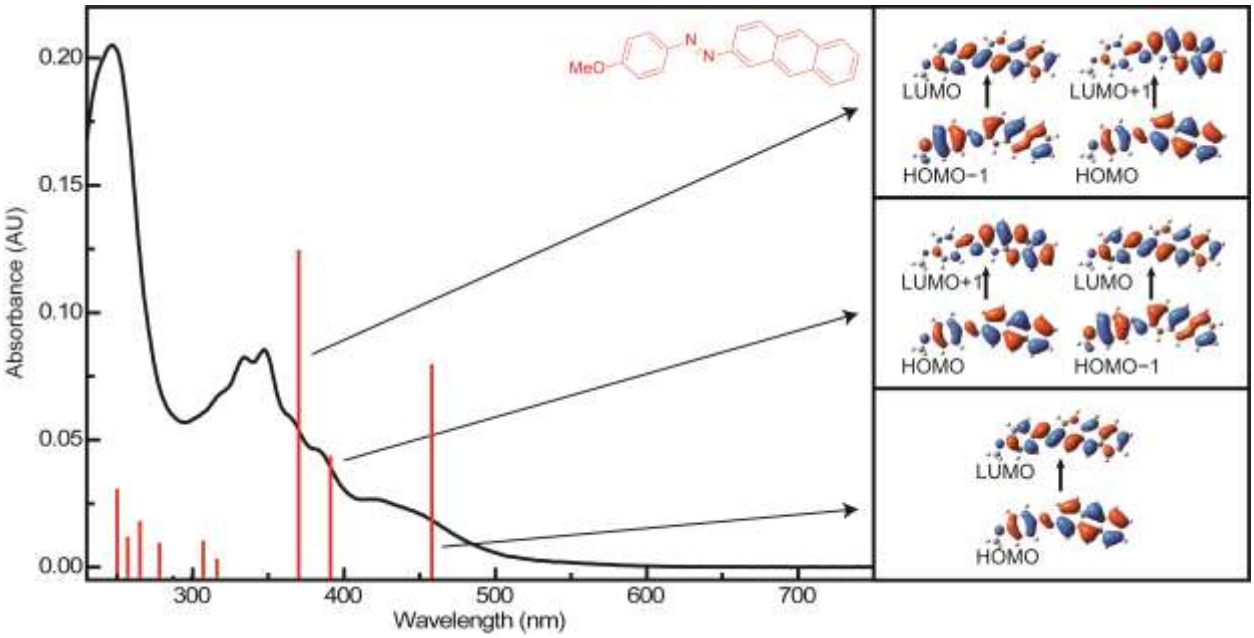

Figure S15: TDDFT transitions for azo-OMe overlaid on its absorption spectrum.

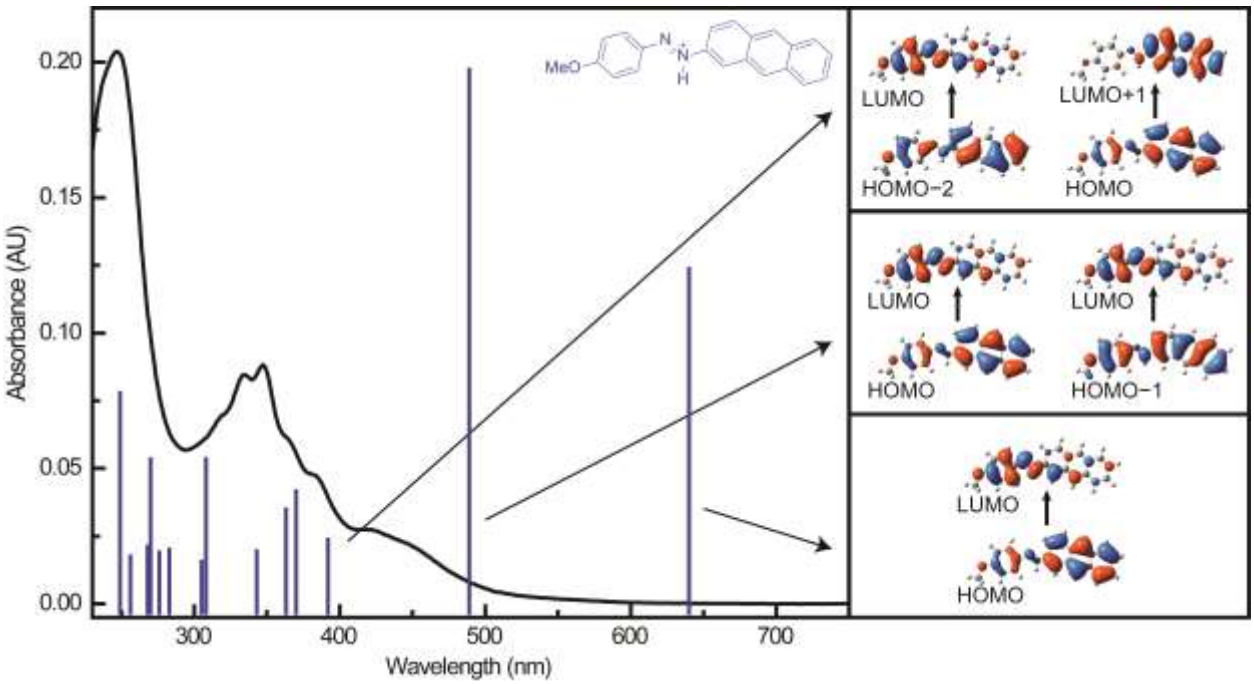

Figure S16: TDDFT transitions for azo-OMe N(2)H overlaid on the absorption spectrum of azo-OMe with 1 eq of trifluoroacetic acid.

Experimental Details

Instrumentation

^{1}H spectra were recorded on a 400 MHz Bruker NMR spectrometer using the residual resonance of the solvent as the internal standard. Chemical shifts are reported in parts per million (ppm). When peak multiplicities are given, the following abbreviations are used: s, singlet; d, doublet; t, triplet; m, multiplet. Molar absorptivity was acquired with Cary 5000 UV-vis-NIR spectrometer. Fluorescence spectra were acquired with a BH Chronos steady-state fluorimeter. ATR-FT-IR data was obtained with a Thermo Scientific Nicolet iS10 with an attenuated total reflectance (ATR) attachment.

Absorption Spectroscopy

Solutions of a known concentration of azo-OH and azo-OMe were prepared in a 10 mL volumetric flask and used to prepare diluted solutions for molar absorptivity experiments. Samples were prepared under ambient conditions and the diluted solutions were at concentrations such that the optical density of each sample was kept below 1 AU for each UV-visible spectrum in a 1-cm quartz cuvette.

Emission Quantum Yields

Emission quantum yields were obtained using solutions of known concentration for both azo-OH and azo-OMe with 0 and 1 eq of TFA added. Reported values are averages of 3 sets of measurements. All measurements were performed on samples at or below 0.1 AU with 1 mm excitation slits and 0.5 mm emission slits for emission spectra. Samples and fluorescence standards were excited at 340 nm. All samples were degassed before measurement in acetonitrile which was dried on 3 Å sieves for 24 hours prior to use.

Cyclic Voltammetry

Cyclic voltammetry (CV) and differential pulse voltammetry (DPV) were acquired with a CH Instruments potentiostat/galvanostat. A 2-mm Pt disk working electrode, Pt wire counter electrode, and Ag wire quasi-reference electrode were used with a ferrocene internal standard. $TBAPF_6$ was recrystallized 3 times from ethanol and dried prior to use. Acetonitrile was dried over CaH_2 and distilled. Dried acetonitrile was stored over 4 Å sieves. Samples were prepared with ≈ 0.5 mM of analyte and 100 mM of $TBAPF_6$ as electrolyte in acetonitrile. Solutions were sparged with N_2 for 5 mins prior to and in between runs and blanketed with N_2 during. All potentials are reported vs $Fc^{+/0}$ couple.

Spectroelectrochemistry

Spectroelectrochemical measurements were recorded with a CH Instruments potentiostat/galvanostat and a USB 2000+ Ocean Optics UV-visible spectrometer with an Analytical Instrument Systems, Inc AIS Model DT 1000 light source. Samples were prepared with a concentration of ≈ 100 µM in acetonitrile with a 100 mM $TBAPF_6$ electrolyte concentration and sparged with N_2. A platinum

mesh working electrode, a silver wire reference electrode, and a platinum wire counter electrode were used. The spectroelectrochemistry cell was constructed in the 2-mm glass cuvette using cleaned and polished electrodes. Bulk electrolysis (BE) was used to apply potential to generate the desired redox product (oxidized or reduced). Prior to BE, the spectrometer was blanked on the sample solution. Absorption spectra were recorded once steady state was reached at each potential step. A series of difference absorption spectra were recorded on each sample. Fresh samples were used for each run.

Transient Absorption

Femtosecond transient absorption spectroscopy was performed with an Ultrafast Systems Helios spectrometer. One hundred fifty femtosecond pulses of 800 nm laser light were generated with a Coherent Libra amplified Ti:sapphire system at 1.2 W and 1 kHz repetition rate. Approximately 80% of the 800 nm pulses was sent to a Topas-C optical parametric amplifier to generate a 370 nm pump pulse. The pump pulse was attenuated to between 0.2 mW and 0.4 mW to prevent decomposition of the sample. The remainder (~20% of the 800 nm light was sent through the sapphire crystal to generate a white light continuum for use as the probe pulse. The probe pulse was delayed on a delay stage to generate every other pump pulse, and for each time delay, a series of unpumped and pumped probe pulses were recorded. In each case, a reference probe pulse (that does not go through the sample) was collected and processed to improve the S/N while minimizing the number of scans needed to obtain quality data. The transient absorption spectra were measured over a 5 ns window. For each scan, 250 time points were recorded and each sample was subjected to three scans. The sample was stirred with a magnetic stir bar during every run. Samples for transient absorption spectroscopy were prepared in a nitrogen environment in a 2-mm quartz high-vacuum cuvette. The concentration of each dyad was 30 μM. UV-visible absorption spectra were recorded before and after each TA experiment to verify that no decomposition had occurred. A chirp correction was applied during analysis of each data set. Data analysis was performed by extracting and retaining 2 principal components and fitting using global analysis software (Ultrafastsystems Surface Xplorer) to isolate decay-associated difference spectra (DADS) and their corresponding lifetimes. Quality of the fitting was assessed by examining the residuals of principle component kinetic traces and the model used to represent the dataset.

Computational Methods

Density functional theory (DFT) and time-dependent density functional theory (TDDFT) calculations were performed on both azo-OH and azo-OMe in the unprotonated state, as well as protonated at either azo bond position. For both azo-OH and azo-OMe, the anthracene moiety-adjacent nitrogen, N(2), was shown to have a lower formal charge. Additionally, the models that were protonated at this position had a lower total energy. For this reason, the N(2)-protonated molecules were chosen for reporting computational results. The B3LYP functional[1–4] and 6-311G basis set[5–8] were used. An acetonitrile solvent environment was simulated with the polarizable continuum model. Molecules were visualized using GaussView 6[9] and calculations were performed using Gaussian 09[10].

Materials and Synthetic Procedures

All reagents were obtained from commercial sources used as received without further purification, unless otherwise specified. Air-sensitive reactions were conducted using a standard Schlenk line techniques under nitrogen. Acetonitrile was dried over CaH_2 and distilled. Dried acetonitrile was stored over 4 Å sieves. Azo-OH and azo-OMe were synthesized using modified procedures.[11,12]

Synthesis of 4-(anthracen-2-yldiazenyl)phenol (azo-OH).

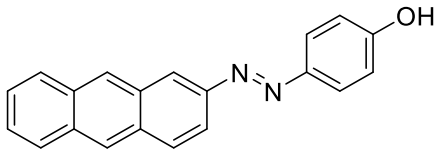

azo-OH

2-aminoanthracene (558 mg, 2.89 mmol) was added to a solution (A) of distilled water (5 mL), acetone (1.2 mL), and concentrated HCl (1 mL). The solution was cooled to 0 °C. A second solution (B) of sodium nitrite (178 mg, 2.58 mmol) in distilled water (6.2 mL) was chilled to 0 °C. Solution B was added slowly to solution A. A third solution (C) of phenol (247 mg, 2.62 mmol) and potassium carbonate (908 mg, 6.57 mmol) in 0.5 M NaOH (6.2 mL) was prepared and cooled to 0 °C. Solution C was slowly added to solution A and stirred at 0 °C for one hour. The reaction was then raised to room temperature and acidified with concentrated HCl. The precipitate was collected by filtration and washed with water and ether. (Yield 56%) ^{1}H NMR (400 MHz, DMSO) δ 10.36 (s, 1H), 8.81 (s, 1H), 8.64 (s, 2H), 8.25 – 8.05 (m, 3H), 8.00 (d, *J* = 9.1 Hz, 1H), 7.88 (d, *J* = 8.8 Hz, 2H), 7.59 (d, *J* = 9.7 Hz, 2H), 6.99 (d, *J* = 8.8 Hz, 2H). ^{13}C NMR (126 MHz, DMSO) δ 160.99, 149.21, 145.40, 132.13, 131.73, 131.12, 129.75, 128.18, 128.15, 126.46, 126.43, 126.21, 124.86, 116.15, 116.03 ESI-MS experimental (calculated) m/z: 299.2 (299.12) $[azo\text{-}OH + H]^+$, 321.2 (321.10) $[azo\text{-}OH + H]^+$

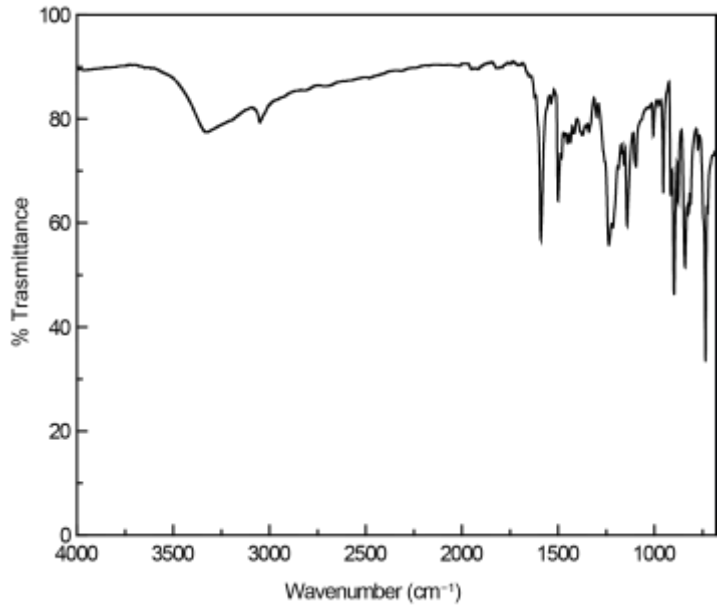

Figure S17. ATR-FT-IR of azo-OH.

Synthesis of (anthracen-2-yl)-2-(4-methoxyphenyl)diazene (azo-OMe).

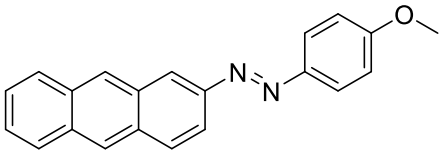

azo-OMe

A schlenk flask with 25 mL of dry acetone was charged with azo-OH (200 mg, 0.7 mmol), MeI (205 µL, 1.68 mmol), potassium carbonate (252 mg, 1.82 mmol), and 18-crown-6 (39 mg, 0.15 mmol). The solution was refluxed under air-free conditions for 24 h. The reaction was cooled to room temperature and the solvent was removed via rotary evaporator. The residue was dissolved in dichloromethane (25 mL) and washed with water (3 × 25 mL). The organic layer was dried with $MgSO_4$ and filtered. The solvent was removed under reduced pressure and recrystallized with dichloromethane/hexanes. (Yield 35%) ^{1}H NMR (400 MHz, $CDCl_3$) δ 8.59 (d, J = 4.6 Hz, 2H), 8.45 (s, 1H), 8.12 – 7.96 (m, 6H), 7.52 (d, J = 9.7 Hz, 2H), 7.06 (d, J = 9.0 Hz, 2H), 3.92 (s, 3H). ^{13}C NMR (126 MHz, $CDCl_3$) δ 162.19, 150.08, 147.37, 132.75, 132.36, 132.29, 131.78, 129.67, 128.45, 128.43, 128.40, 126.61, 126.32, 126.02, 124.89, 116.82, 114.43, 55.77 ESI-MS experimental (calculated) m/z: 313.1 (313.13) [azo-OMe + H]+, 335.0 (335.12) [azo-OMe + H]+

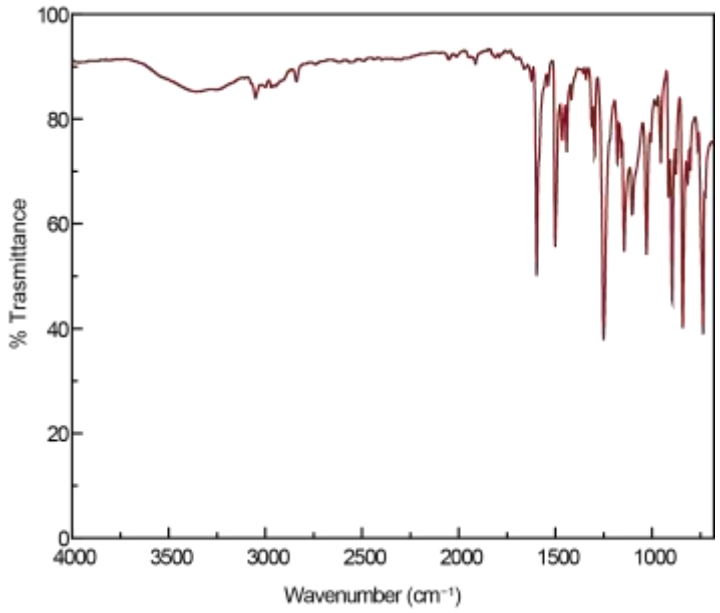

Figure S18. ATR-FT-IR of azo-OMe.

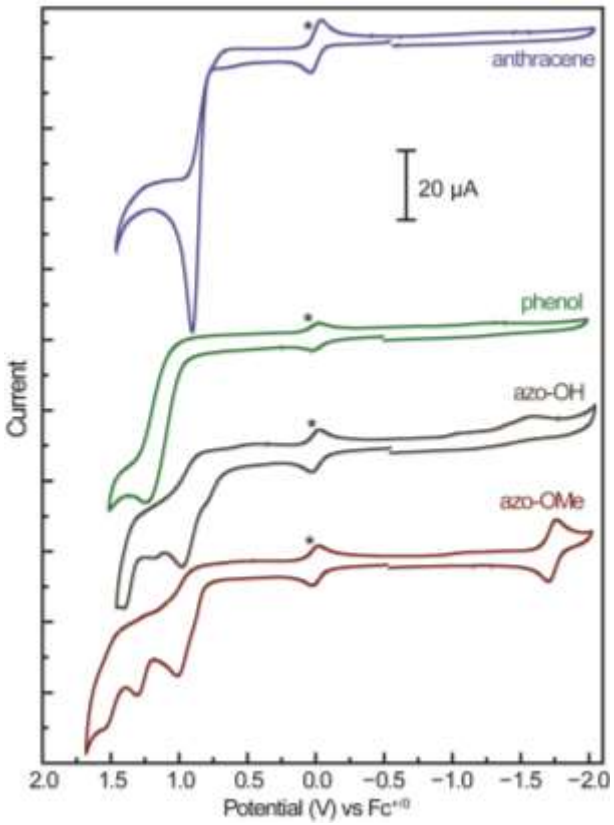

Figure S19. Cyclic voltammograms of 0.5 mM anthracene, phenol, azo-OH, and azo-OMe in 100 mM $TBAPF_6$ in acetonitrile at scan rate = 100 mV/s. The star notes $Fc^{+/0}$ couple.

TDDFT Data Tables

azo-OH

Excited State	Energy (eV)	Wavelength (nm)	Oscillator Strength	From MO number	To MO number	Transition Contribution
1	2.6398	469.67	f=0.0000	76	79	0.68091
				76	80	0.17442
2	2.7147	456.72	f=0.5323	77	79	0.11483
				78	79	0.69013
3	3.2003	387.42	f=0.2300	75	79	-0.12902
				77	79	0.50233
				78	79	-0.13554
				78	80	0.45244
4	3.3882	365.93	f=1.0659	77	79	-0.4715
				78	80	0.51954
5	3.8877	318.92	f=0.0000	76	79	-0.17663
				76	80	0.67679
6	3.9634	312.82	f=0.0090	75	79	0.56044
				77	80	-0.38588
7	4.0623	305.2	f=0.0493	75	79	0.22823
				75	80	-0.11967
				77	80	0.50761
				78	81	-0.28319
				78	82	-0.25271
8	4.1711	297.25	f=0.0037	73	79	-0.26579
				74	79	0.58352
				77	81	-0.12168
				78	82	-0.18478
9	4.3367	285.89	f=0.0027	73	79	0.58976
				74	79	0.28637
				75	80	0.13916
				78	83	0.16291
10	4.5003	275.5	f=0.0610	73	79	-0.11032
				75	79	0.25481
				75	80	0.48297
				77	80	0.22217
				77	82	0.13069

				78	81	0.26081
				78	82	0.1396
11	4.6605	266.03	f=0.1025	74	79	-0.19764
				75	80	-0.12566
				78	81	0.49064
				78	82	-0.4198
12	4.8359	256.38	f=0.0754	73	79	-0.16131
				73	80	-0.11411
				74	80	-0.12743
				75	80	0.19932
				78	81	-0.15337
				78	82	-0.14058
				78	83	0.57622
13	4.9906	248.43	f=0.2640	71	79	0.12245
				73	80	0.42496
				74	80	0.41544
				75	79	-0.10771
				75	80	0.10832
				77	80	-0.11282
				78	81	-0.1134
				78	82	-0.23075
14	4.9931	248.31	f=0.0000	76	81	0.64705
				76	82	-0.27994
15	5.0882	243.67	f=0.1411	73	80	0.18979
				74	79	0.1165
				74	80	-0.3783
				75	80	0.12687
				77	81	0.40799
				77	82	-0.15287
				78	82	-0.19686
				78	83	-0.18864
16	5.1485	240.82	f=0.5763	72	79	0.15348
				73	80	0.41206
				74	80	-0.14879
				75	79	0.11153
				75	80	-0.27058
				77	80	0.10686
				77	82	-0.11763
				78	81	0.1856
				78	82	0.22895
				78	83	0.25504
17	5.2366	236.77	f=0.0002	76	81	0.27357

				76	82	0.6312
				76	83	0.11087
18	5.2588	235.76	f=0.1013	72	79	0.2911
				73	80	-0.17031
				74	80	0.27467
				75	80	-0.17417
				77	81	0.47475
				78	84	-0.10154
19	5.2998	233.94	f=0.0845	71	79	0.47008
				72	79	-0.19899
				73	80	-0.12093
				75	80	-0.12381
				77	81	0.14334
				78	84	0.3881
20	5.3489	231.79	f=0.1013	72	79	0.21987
				73	80	0.10347
				74	80	-0.21757
				77	82	0.56363
21	5.4056	229.36	f=0.0798	71	79	0.28763
				72	79	0.46444
				75	80	0.10798
				77	81	-0.1435
				77	82	-0.24174
				77	83	0.22014
				78	83	-0.10937
				78	85	0.13344
22	5.6079	221.09	f=0.0001	76	82	-0.11738
				76	83	0.67079
				76	84	0.13542
23	5.646	219.6	f=0.0052	71	79	-0.34087
				71	80	-0.18614
				72	79	0.10742
				72	80	0.10149
				77	83	0.29106
				77	84	0.10647
				78	84	0.42903
				78	85	-0.12551
24	5.6648	218.87	f=0.0201	71	79	0.17324
				71	80	0.12592
				72	79	-0.11806
				77	82	0.132
				77	83	0.49318

				78	84	-0.23901
				78	85	-0.25751
25	5.7973	213.87	f=0.0000	70	79	0.66475
				70	80	-0.17832

azo-OH N(2)H

Excited State	Energy (eV)	Wavelength (nm)	Oscillator Strength	From MO number	To MO number	Transition Contribution
1	1.8114	684.47	f=0.4314	77	79	-0.13052
				78	79	0.69543
2	2.6849	461.79	f=0.9270	76	79	-0.15604
				77	79	0.67118
				78	79	0.13996
3	3.1955	387.99	f=0.2935	75	79	-0.10133
				76	79	0.44504
				77	79	0.16249
				78	80	0.50371
4	3.3252	372.87	f=0.0243	75	79	0.1801
				76	79	-0.46874
				78	80	0.47624
5	3.5375	350.48	f=0.0077	74	79	0.57067
				75	79	-0.39777
6	3.7463	330.95	f=0.1928	74	79	0.38458
				75	79	0.52256
				76	79	0.18827
				77	80	-0.13321
7	3.9591	313.16	f=0.0304	76	80	-0.12878
				77	80	0.52525
				78	81	-0.13886
				78	82	0.41397
8	4.0953	302.75	f=0.0013	71	79	0.69294
9	4.4061	281.39	f=0.0476	73	79	-0.38194
				78	81	0.56038
10	4.4168	280.71	f=0.0279	73	79	0.56693
				78	81	0.38621
11	4.5099	274.92	f=0.0438	72	79	-0.12414
				76	80	0.5173
				77	80	0.2799
				78	82	-0.23575
				78	83	0.24693

12	4.6683	265.58	f=0.0328	72	79	0.66679
				78	84	-0.10695
13	4.8221	257.12	f=0.0285	75	80	-0.13688
				76	80	-0.16679
				77	80	-0.16084
				78	83	0.62108
14	4.9649	249.72	f=0.7089	75	80	0.39168
				76	80	-0.31748
				77	80	0.23931
				78	82	-0.35325
				78	83	0.10637
15	5.0116	247.39	f=0.0000	67	79	-0.11586
				70	79	0.68146
				71	79	0.10716
16	5.1564	240.45	f=0.4136	75	80	0.47754
				76	80	0.19585
				77	80	-0.109
				77	81	-0.24297
				78	82	0.28791
				78	83	0.1145
				78	84	-0.18608
17	5.2633	235.57	f=0.0335	74	80	0.13158
				74	84	0.10247
				75	80	0.12748
				77	81	0.615
				78	82	0.14321
18	5.3698	230.89	f=0.0001	69	79	0.68813
19	5.4569	227.2	f=0.1516	73	80	-0.12302
				74	80	-0.2196
				75	80	0.15228
				76	80	0.10867
				77	83	0.20426
				78	84	0.54383
				78	85	0.16168
20	5.486	226	f=0.0462	74	80	0.48521
				76	82	0.11528
				77	81	-0.10534
				77	82	0.36263
				78	84	0.27508
21	5.5087	225.07	f=0.0175	73	80	0.19691
				74	80	-0.36819
				76	82	0.11725

				77	82	0.38104
				77	83	-0.15122
				78	84	0.10729
				78	85	-0.30927
22	5.5456	223.57	f=0.0000	66	79	0.65674
				67	79	0.23871
23	5.5671	222.71	f=0.0167	73	80	-0.27157
				74	80	-0.23219
				75	80	-0.14665
				77	82	0.16264
				77	83	-0.23273
				78	84	-0.10356
				78	85	0.46413
24	5.6847	218.1	f=0.0000	66	79	-0.2339
				67	79	0.643
				70	79	0.10574
25	5.7546	215.45	f=0.0910	68	79	0.41691
				74	81	0.11783
				76	82	-0.22968
				77	82	0.25692
				77	83	0.32658
				78	84	-0.15315

azo-OMe

Excited State	Energy (eV)	Wavelength (nm)	Oscillator Strength	From MO number	To MO number	Transition Contribution
1	2.6307	471.29	f=0.0000	80	83	0.68129
				80	84	0.17291
2	2.7043	458.48	f=0.5864	81	83	0.10772
				82	83	0.6911
3	3.1721	390.86	f=0.3312	79	83	-0.12363
				81	83	0.55472
				82	83	-0.13416
				82	84	0.38907
4	3.3538	369.68	f=0.9058	81	83	-0.41084
				82	84	0.56753
5	3.8797	319.57	f=0.0000	80	83	-0.17507
				80	84	0.67722
6	3.9257	315.82	f=0.0190	79	83	0.55368
				81	84	-0.39824

				82	85	-0.10052
7	4.0373	307.1	f=0.0759	77	83	0.10277
				79	83	0.2486
				79	84	-0.10758
				81	84	0.50664
				82	85	-0.31322
				82	86	-0.17728
8	4.1498	298.77	f=0.0046	77	83	-0.21461
				78	83	0.60208
				81	85	-0.10644
				82	86	-0.21247
9	4.3265	286.57	f=0.0050	77	83	0.60827
				78	83	0.24657
				79	84	0.13957
				82	87	0.1636
10	4.4656	277.64	f=0.0702	77	83	-0.12242
				79	83	0.2571
				79	84	0.47844
				81	84	0.21453
				81	86	0.12396
				82	85	0.29046
				82	86	0.11237
11	4.6761	265.14	f=0.1363	78	83	0.19481
				79	84	0.13006
				82	85	-0.42687
				82	86	0.48145
12	4.8269	256.86	f=0.0874	77	83	-0.16745
				77	84	-0.13043
				78	84	-0.15286
				79	84	0.20494
				82	85	-0.17608
				82	86	-0.12992
				82	87	0.55647
13	4.9714	249.39	f=0.2266	75	83	0.11918
				77	84	0.41006
				78	84	0.44403
				82	85	-0.14218
				82	86	-0.20295
14	5.0144	247.25	f=0.0000	80	85	0.62728
				80	86	-0.32023
15	5.0656	244.76	f=0.1940	77	84	0.17362
				78	84	-0.32467

				79	84	0.16288
				81	85	0.37925
				81	86	-0.17774
				82	86	-0.24304
				82	87	-0.24493
16	5.1271	241.82	f=0.4248	76	83	0.18131
				77	84	0.43146
				78	84	-0.22087
				79	84	-0.23316
				81	86	-0.14462
				82	85	0.20147
				82	86	0.15767
				82	87	0.23146
17	5.2213	237.46	f=0.1443	76	83	0.31754
				77	84	-0.16603
				78	84	0.21104
				79	84	-0.1983
				81	85	0.49301
18	5.2395	236.63	f=0.0002	80	85	0.31199
				80	86	0.61219
				80	87	0.11967
19	5.2965	234.09	f=0.0956	75	83	0.48935
				75	84	-0.10593
				76	83	-0.16533
				77	84	-0.10001
				79	84	-0.1207
				81	85	0.11653
				82	88	0.39164
20	5.321	233.01	f=0.0600	76	83	0.23188
				77	84	0.10925
				78	84	-0.24132
				81	86	0.54926
				82	85	-0.1013
21	5.3709	230.84	f=0.1473	75	83	0.24678
				76	83	0.4564
				79	84	0.13856
				81	85	-0.17476
				81	86	-0.25757
				81	87	0.20529
				82	87	-0.13283
				82	89	0.10884
22	5.6016	221.34	f=0.0001	80	86	-0.12233

				80	87	0.66906
				80	88	0.13471
23	5.6288	220.27	f=0.0275	75	83	-0.14781
				77	84	0.1009
				81	86	0.10943
				81	87	0.55817
				82	88	0.1701
				82	89	-0.23082
24	5.6491	219.48	f=0.0046	75	83	-0.37088
				75	84	-0.2228
				76	83	0.11976
				76	84	0.11029
				81	87	-0.1976
				82	88	0.4588
25	5.7952	213.94	f=0.0000	70	83	0.10445
				72	83	-0.12055
				73	83	0.65372
				73	84	-0.16563

azo-OMe N(2)H

Excited State	Energy (eV)	Wavelength (nm)	Oscillator Strength	From MO number	To MO number	Transition Contribution
1	1.8127	683.98	f=0.4652	81	83	-0.1252
				82	83	0.69613
2	2.6605	466.02	f=0.9869	80	83	-0.15335
				81	83	0.67338
				82	83	0.13612
3	3.1811	389.75	f=0.2663	79	83	0.10561
				80	83	0.45568
				81	83	0.15501
				82	84	0.49312
4	3.3189	373.57	f=0.0221	78	83	0.11106
				79	83	-0.15341
				80	83	-0.4572
				82	84	0.48945
5	3.496	354.65	f=0.0105	78	83	0.47743
				79	83	0.50654
6	3.7215	333.16	f=0.1674	78	83	0.48619
				79	83	-0.43332
				80	83	0.19002

				81	84	-0.1304
7	3.9466	314.15	f=0.0322	80	84	-0.14323
				81	84	0.5268
				82	85	0.18719
				82	86	0.38646
8	4.0805	303.85	f=0.0013	75	83	0.69228
9	4.4194	280.54	f=0.0146	76	83	-0.10607
				77	83	0.61498
				80	84	-0.18903
				81	84	-0.12309
				82	85	0.21368
10	4.4438	279	f=0.1116	77	83	-0.25246
				81	84	-0.12671
				82	85	0.61868
				82	86	-0.14011
11	4.4801	276.74	f=0.0230	76	83	-0.13179
				77	83	0.13875
				80	84	0.48286
				81	84	0.26941
				82	85	0.1053
				82	86	-0.28512
				82	87	0.22014
12	4.6038	269.31	f=0.0537	76	83	0.66229
				77	83	0.13231
13	4.8033	258.12	f=0.0313	79	84	0.19791
				80	84	-0.12622
				81	84	-0.1592
				82	87	0.61773
14	4.9482	250.57	f=0.5542	79	84	0.43972
				80	84	0.30262
				81	84	-0.19114
				82	86	0.30966
				82	87	-0.16352
15	5.0238	246.8	f=0.0000	70	83	-0.11287
				74	83	0.68444
16	5.1228	242.02	f=0.5168	79	84	0.43244
				80	84	-0.24296
				81	84	0.11754
				81	85	-0.25234
				82	86	-0.31512
				82	87	-0.13724

				82	88	0.16287
17	5.1313	241.62	f=0.0001	72	83	0.64748
				73	83	-0.23197
18	5.2522	236.06	f=0.0329	78	84	-0.13027
				78	88	-0.10067
				79	84	0.11111
				80	84	-0.11331
				81	85	0.60761
				82	86	-0.13773
19	5.3829	230.33	f=0.0001	72	83	0.22577
				73	83	0.65113
20	5.4304	228.32	f=0.0932	78	84	0.39908
				79	84	0.1554
				80	84	-0.1143
				81	86	0.231
				81	87	-0.20301
				82	88	-0.38557
21	5.4628	226.96	f=0.1174	78	84	0.27614
				81	86	0.34912
				82	88	0.49772
22	5.4868	225.97	f=0.0319	71	83	-0.13357
				77	84	-0.16849
				78	84	0.41873
				81	86	-0.36698
				81	87	0.15643
				82	89	0.27722
23	5.5435	223.66	f=0.0253	71	83	0.43252
				77	84	-0.26498
				78	84	-0.17061
				82	89	0.41359
24	5.57	222.59	f=0.0040	71	83	0.49917
				77	84	0.15134
				78	84	0.17402
				81	86	-0.12219
				81	87	0.22745
				82	89	-0.28514
25	5.6903	217.89	f=0.0000	70	83	0.68381
				74	83	0.10608

1 F. J. Devlin, J. W. Finley, P. J. Stephens and M. J. Frisch, *J. Phys. Chem.*, 1995, **99**, 16883–16902.

2 L. S. Kassel, *J. Chem. Phys.*, 1936, **4**, 276–282.

3 A. D. Becke, *J. Chem. Phys.*, 1993, **98**, 5648–5652.

4 C. Lee, C. Hill and N. Carolina, *Chem. Phys. Lett.*, 1989, **162**, 165–169.

5 R. Ditchfield, W. J. Hehre and J. A. Pople, *J. Chem. Phys.*, 2004, **54**, 724–728.

6 M. M. Francl, W. J. Pietro, W. J. Hehre, J. S. Binkley, M. S. Gordon, D. J. DeFrees and J. A. Pople, *J. Chem. Phys.*, 1982, **77**, 3654–3665.

7 W. J. Hehre, K. Ditchfield and J. A. Pople, *J. Chem. Phys.*, 1972, **56**, 2257–2261.

8 P. C. Hariharan and J. A. Pople, *Theor. Chim. Acta*, 1973, **28**, 213–222.

9 R. Dennington, T. Keith and J. Millam, 2016, GaussView, Semichem Inc., Shawnee Mission, KS.

10 M. J. Frisch, G. W. Trucks, H. B. Schlegel, G. E. Scuseria, M. A. Robb, J. R. Cheeseman, G. Scalmani, V. Barone, G. A. Petersson, H. Nakatsuji, X. Li, M. Caricato, A. V. Marenich, J. Bloino, B. G. Janesko, R. Gomperts, B. Mennucci, H. P. Hratchian, J. V. Ortiz, A. F. Izmaylov, J. L. Sonnenberg, D. Williams-Young, F. Ding, F. Lipparini, F. Egidi, J. Goings, B. Peng, A. Petrone, T. Henderson, D. Ranasinghe, V. G. Zakrzewski, J. Gao, N. Rega, G. Zheng, W. Liang, M. Hada, M. Ehara, K. Toyota, R. Fukuda, J. Hasegawa, M. Ishida, T. Nakajima, Y. Honda, O. Kitao, H. Nakai, T. Vreven, K. Throssell, J. J. A. Montgomery, J. E. Peralta, F. Ogliaro, M. J. Bearpark, J. J. Heyd, E. N. Brothers, K. N. Kudin, V. N. Staroverov, T. A. Keith, R. Kobayashi, J. Normand, K. Raghavachari, A. P. Rendell, J. C. Burant, S. S. Iyengar, J. Tomasi, M. Cossi, J. M. Millam, M. Klene, C. Adamo, R. Cammi, J. W. Ochterski, R. L. Martin, K. Morokuma, O. Farkas, J. B. Foresman and D. J. Fox, 2016, Gaussian 16, Gaussian, Inc., Wallingford CT.

11 D. Abdallah, J. Whelan, J. M. Dust, S. Hoz and E. Buncel, *J. Phys. Chem. A*, 2009, **113**, 6640–6647.

12 S. Concilio, L. Sessa, A. M. Petrone, A. Porta, R. Diana, P. Iannelli and S. Piotto, *Molecules*, 2017, **22**, 875.